Article

Optimum Application of Thermal Factors to Artificial Neural Network Models for Improvement of Control Performance in Double Skin-Enveloped Buildings

Jin Woo Moon [1], Kyung-Il Chin [2] and Sooyoung Kim [3],*

[1] Department of Building & Plant Engineering, Hanbat National University, Daejeon 305-719, Korea; E-Mail: jwmoon@hanbat.ac.kr

[2] Department of Architectural Engineering, Hanbat National University, Daejeon 305-719, Korea; E-Mail: classic9@naver.com

[3] Department of Interior Architecture & Built Environment, Yonsei University, Seoul 120-749, Korea

* Author to whom correspondence should be addressed; E-Mail: sooyoung@yonsei.ac.kr; Tel.: +82-2-2123-3142; Fax: +82-2-313-3139.

Abstract: This study proposes an artificial neural network (ANN)-based thermal control method for buildings with double skin envelopes that has rational relationships between the ANN model input and output. The relationship between the indoor air temperature and surrounding environmental factors was investigated based on field measurement data from an actual building. The results imply that the indoor temperature was not significantly influenced by vertical solar irradiance, but by the outdoor and cavity temperature. Accordingly, a new ANN model developed in this study excluded solar irradiance as an input variable for predicting the future indoor temperature. The structure and learning method of this new ANN model was optimized, followed by the performance tests of a variety of internal and external envelope opening strategies for the heating and cooling seasons. The performance tests revealed that the optimized ANN-based logic yielded better temperature conditions than the non-ANN based logic. This ANN-based logic increased overall comfortable periods and decreased the frequency of overshoots and undershoots out of the thermal comfort range. The ANN model proved that it has the potential to be successfully applied in the temperature control logic for double skin-enveloped buildings. The ANN model, which was proposed in this study, effectively predicted future indoor temperatures for the diverse opening strategies. The ANN-based logic optimally

determined the operation of heating and cooling systems as well as opening conditions for the double skin envelopes.

Keywords: double skin envelope; temperature control logic; artificial neural network; predictive and adaptive controls; model optimization

Nomenclature:

$TEMP_{IN}$	Indoor air temperature (°C)
$\Delta TEMP_{IN}$	Indoor air temperature change from the preceding cycle (°C)
$TEMP_{OUT}$	Outdoor air temperature (°C)
$TEMP_{CAV}$	Cavity air temperature (°C)
$TEMP_{PR}$	Indoor air temperature change predicted by the ANN model (°C)
N_i	Number of neurons in the input layer
N_h	Number of neurons in the hidden layer
N_o	Number of neurons in the output layer
N_d	Number of training data sets

1. Introduction

A double skin envelope (DSE) has been applied to buildings constructed with curtain wall structures. This is due to the resulting improved insulation capability, utilization of solar energy and control of energy flow, features which are rarely available in single-skinned buildings. It is well known that solar energy accumulated in the cavity formed between the internal and external skins functions to effectively reduce heating energy utilization in the winter when the openings installed in the envelopes are controlled appropriately [1–4]. Not only the proper operation of the openings, but also the operation of the shading devices is critical to improve building energy-efficiency. From this point of view, an integrated glass-shading device system on the external was developed for reducing heating and cooling loads by controlling the amount of solar incidence. In comparative performance tests with traditional building enclosures, the double skin envelope with the proposed shading device system proved its superiority in building energy behavior [5].

Diverse ventilation strategies involving the openings in the double skin envelopes have been investigated to identify more energy efficient control methods. For example, rule-based and optimal theory-based controls were proposed to control openings in the internal and external envelopes of buildings [6,7]. Rule-based control methods are more frequently applied in actual buildings due to the simplicity of the required control algorithms and devices.

However, previous studies have revealed some limitations of the rule-based methods [1,2,8,9]. An effective temperature control logic based on an artificial neural network (ANN) was proposed in these studies in order to improve the intuitiveness of the rules in the logic of rule-based methods. The different types of control logic used for heating and cooling seasons are shown in Figure 1, where the ANN model was employed for predictive and adaptive controls.

Two fundamental rules are engaged in the control logic. First, the operation of the openings of the internal and external envelopes is determined based on the ANN predictions (TEMP$_{PRE}$) for 4-opening strategies in the 1st step of the Figure 1. For example, the optimal opening strategy in the winter is the way that the future indoor temperature will be highest.

Second, the operation of the heating and cooling systems is determined by the comparison between the TEMP$_{IN}$ + TEMP$_{PRE}$ and the specified operating ranges in the 2nd and 3rd steps of the Figure 1. For example, when the heating system is working and TEMP$_{IN}$ + TEM$_{PRE}$ is over the upper limit of heating range, a heating system stops working at the current cycle.

Figure 1. Integrated temperature control logic for buildings with double skin envelopes [1,2,8,10]. (**a**) Control logic for heating season; (**b**) Control logic for cooling season.

(**a**)   (**b**)
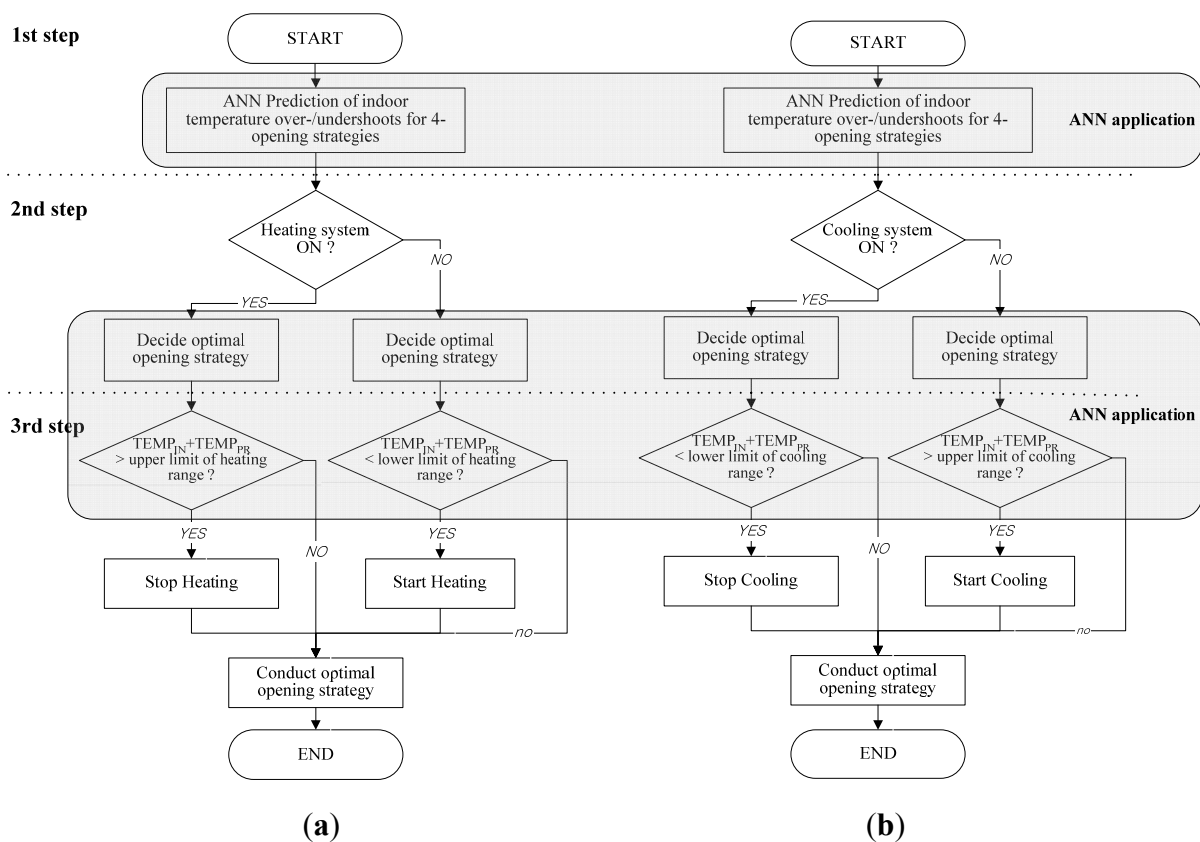
The ANN model developed in previous studies predicted future indoor temperature conditions based on a series of inputs such as the indoor temperature, indoor temperature changes from the preceding control cycle, outdoor and cavity temperature, solar irradiance through the vertical surface, and the opening conditions of the internal and external envelopes. A control cycle means a repeated cycle in the control loop based on which the conditions of the thermal factors are monitored and the signals for system operation are determined. The time frame of cycle in the previous and this study was 1 min.

Specifically, the ANN model predicted future indoor temperature conditions under four combined internal and external envelope opening options. The predicted future temperature of the indoor space under the four combined opening options was compared using control logic in order to determine the optimum method to control the openings in the installed envelopes. Based on the results obtained from

the control logic, optimal control strategies for the openings as well as the operation of heating and cooling systems were determined.

The indoor temperature profile provided by the ANN-based control logic is conceptually illustrated in Figure 2. Since the working conditions of the heating and cooling systems are predetermined before the indoor temperature reached or went beyond the operating range, the indoor temperature could be more stably maintained within the designated thermal comfort range. The performance tests conducted in previous studies implied that the ANN models had acceptable prediction accuracy for temperature variation [1,2,8,10]. This result led to the conclusion that the control logic and ANN model have strong potential for predicting future temperature variation in buildings with double skin envelopes.

Figure 2. Conceptual profile of indoor temperature by ANN-based logic for heating and cooling season.
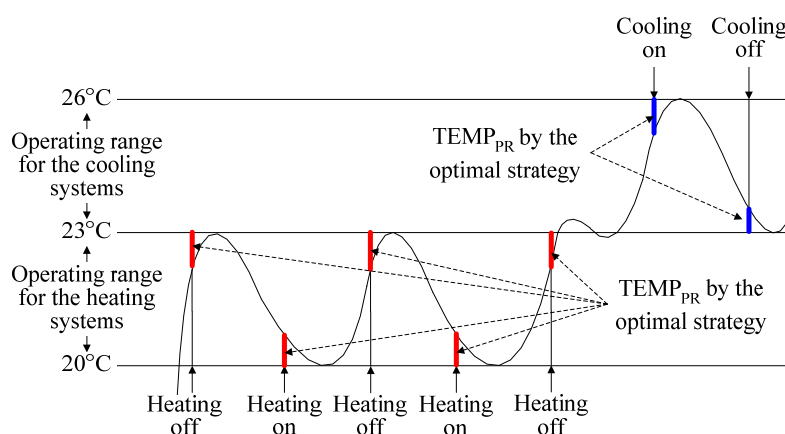
Although the results of previous studies suggested advancement in thermal control for buildings, the ANN-based method, which was developed in the previous study, had limitations in predicting the indoor temperature. The input variables used in the ANN model were intuitively selected without substantial verification of their relationship with the output. The indoor, outdoor and cavity temperatures as well as the amount of solar irradiance were assumed to have a significant effect on the future indoor temperature based on a general understanding. Thus, since the scientific rationality for choosing input variables for predicting output variable was not clearly proved, there is a possibility that the previous ANN model provides extraordinary prediction results for future temperature conditions under the assumptions made in previous studies. [1,2,8,10].

The aim of this study was to develop an ANN model based on the relationships between variables used for inputs and outputs in order to resolve the limitations of the previously proposed ANN model under various circumstances. Applying the ANN model having a structural relationship with the temperature control logic is expected to enable more efficient control of envelope openings and temperature control device operation in order to maintain a more comfortable indoor thermal environment.

This study employs three research phases to achieve the research objectives. First, the relationship between indoor air temperature conditions and other environmental factors such as outdoor and cavity temperatures and the amount of solar irradiance that reaches vertical surfaces were statistically examined. A new ANN model comprised of environmental factors significantly correlated with the indoor temperature as the input variables was subsequently developed.

Next, the structure and learning methods of this new ANN model were parametrically optimized in terms of the prediction accuracy. The difference between the predicted values from the ANN model and the measured values from an actual building was compared for the optimization phase. Finally, performance tests of the optimized ANN model were conducted for various control options, which were combined with the conditions of openings installed in the internal and external envelopes of an actual building.

2. Determination of Relationships between Thermal Factors

Indoor air temperature conditions are derived by heat transfer processes such as conduction through the envelope, ventilation and infiltration rates, solar radiation, and internal loads. The relative factors associated with the heat transfer process through a double skin envelope are summarized in Figure 3. Indoor, outdoor and cavity air temperatures, solar irradiance, people, lighting and equipment indoors, surface opening conditions, and the size and properties of envelope components determine the amount of heat transferred between the indoor space and outdoor environment.

**Figure 3.** Influential factors in the variation of indoor temperature conditions.
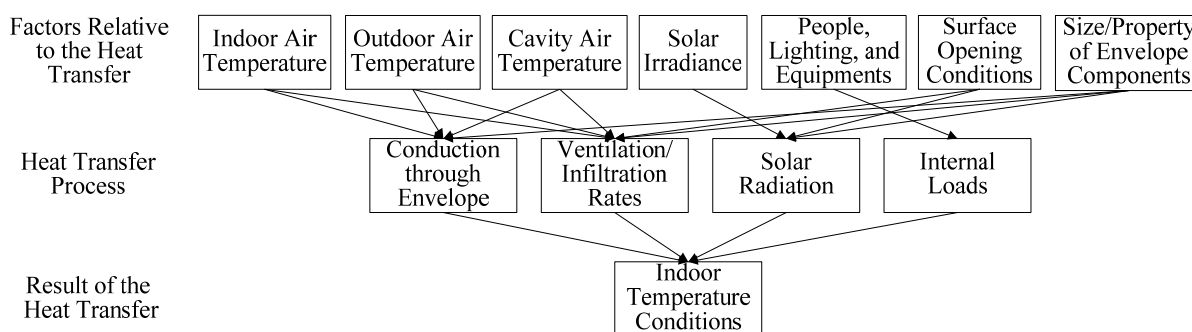
Previous studies [1,2,8,10]. employed the following seven factors as input variables for the ANN model to predict future indoor temperature: (i) current indoor temperature; (ii) degree of indoor temperature change from the preceding control cycle; (iii) outdoor temperature; (iv) cavity temperature; (v) amount of solar irradiance on a vertical surface; (vi) opening conditions of the inner surface; and (vii) opening conditions of the outer surface. These variables were intuitively selected based on the general assumption that all those factors might influence indoor temperature. Thus, analysis of the correlation between inputs and the output of the ANN model needs to be performed in order to select statistically meaningful variables as inputs. In this study, data collected from field measurements in an actual building with a double skin envelope were analyzed to determine the exact relationships among various thermal factors that affect the thermal environment of buildings with double skin envelopes.

2.1. Field Measurement Conditions

Data collection was conducted in an actual double skin enveloped building constructed in Ansan, South Korea (latitude: 37°17' N, longitude: 126°49' E). The building properties and measurement

conditions used for data collection were the same as the conditions used in previous research [3,4]. Figure 4 details the properties of the building.

Figure 4. Layout of tested building and detailed description of cavity space. (**a**) View of building Layout of building; (**b**) Layout of building; (**c**) Section of building; (**d**) Conceptual diagram of air flow in cavity.

(**a**)

(**b**)

(**c**)

(**d**)
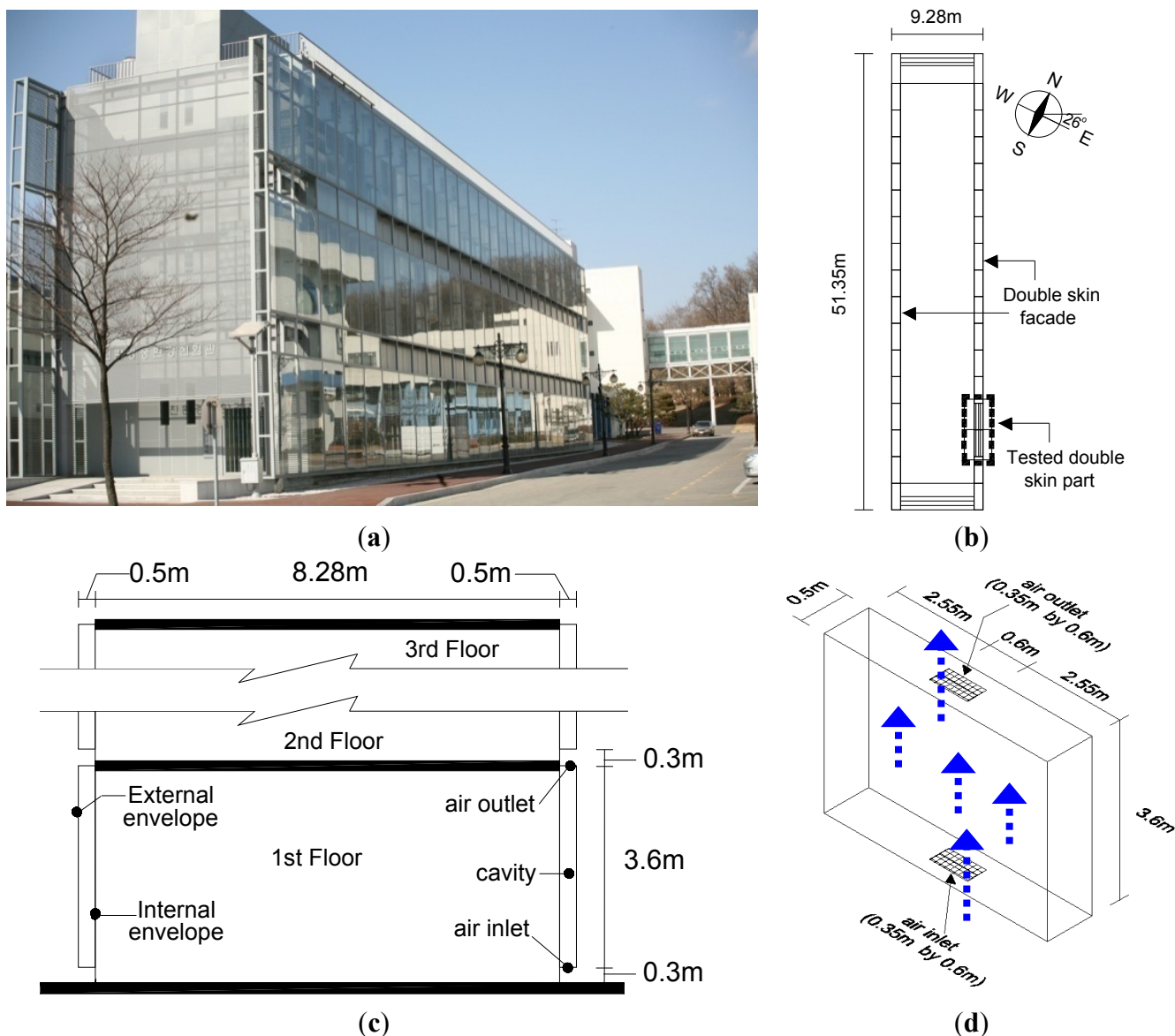
The building was constructed with a curtain wall structure and has three stories with fully covered glazing in its long façades facing east and west. The long axis of the building where the double skin envelope was installed was rotated 26° to the west from the north-south axis. The double skin envelope was installed on the two long main facades marked in Figure 4. The double skin system covered the first floor of the building. Since the internal and external skin was covered with glazing, a cavity space existed between them. During the measurement period, the test double skin module was not occupied by any persons. In addition, no heating and cooling systems were operated for thermal conditioning.

Figure 4 shows the detailed configuration of the cavity space in the double skin envelope. The width, depth and height of the cavity space were 5.7 m, 0.5 m and 3.6 m, respectively. Two 0.6 m

(width) by 0.35 m (depth) openings were installed at the top and bottom. The remaining part of the surface was fully covered with plastic material such that air was only able to pass through the openings. The distance from the ground and the opening at the bottom of the cavity was 0.3 m. The presence of the openings induced air to naturally flow from the bottom and be exhausted through the opening at the top. A conceptual description of the airflow through the cavity space is shown in Figure 4.

The heat transfer coefficients of the glazing used for the external and internal envelopes were 5.88 W/m^2 K and 2.83 W/m^2 K, respectively, which satisfy the national building codes in Korea. The solar heat gain factors for the external and internal envelope were 0.855 and 0.755, respectively. The absorption and reflection coefficients for the external glazing were 0.095 and 0.075 and those for the internal glazing were 0.101 and 0.126. Venetian blinds were installed on the outside of internal envelope in order to control the solar irradiance penetrating through the envelopes. The depth of the slats was 2.54 cm and the distance between each slat was 2.54 cm. During the data monitoring periods, the blind slats remained horizontal and covered the entire outside area of the internal skin.

Data was collected daily for 12 months beginning in December 2007. The monitoring interval was 1 min for the daily data monitoring period, which spanned from 00:00 to 24:00. The air temperature was measured at 80 points, and thermal properties related to the sun, such as irradiance and illuminance, were measured. The data were saved by an automatic data logger system and transferred to a personal computer. The data was classified into three categories, which were clear, partly cloudy and overcast conditions. Selected data are used in this paper to discuss the variation in and relationships among thermal factors.

### 2.2. Relationship among Thermal Factors Based on Field Measurement

A variety of thermal factors that potentially influence indoor temperature were measured from in this study. Among them, some factors were selectively chosen for our discussion of their variation with respect to sky conditions. Figure 5 shows the variation in outdoor horizontal and vertical irradiance under clear (14 February) and overcast (25 February) skies.

Under a clear sky, the horizontal irradiance varied stably over the entire data monitoring period, although very little fluctuation occurred in some cases. This indicates that the sun was not blocked by the clouds, leading to a maximum value of 640.65 W/m^2 with a stable variation pattern. The irradiance on the day when the sky was overcast also showed a stable variation pattern across the days' monitoring intervals. The maximum value was 312.18 W/m^2, which was 48.72% that under clear sky.

The amount of vertical irradiance that reached the easting-facing envelope under the overcast sky showed stable changes. Due to the orientation of the building, the maximum value of 280.57 W/m^2 was observed at 08:59 when the solar azimuth angle was −54.79°. The irradiance decreased steeply until 11:00 and did not exceed 96.26 W/m^2 for the remaining monitored time period, although horizontal irradiance did increase toward the maximum value. The mean ratio of vertical irradiance to horizontal irradiance during the monitored period was 26.21% and 36.92% on a clear and overcast sky, respectively. The vertical irradiance under an overcast sky was lower than that under a clear sky. The difference in vertical irradiance between the clear and overcast skies was greater than that of horizontal irradiance due to the direct irradiance on the east-facing double skin envelope. After 11:00 the vertical irradiance under overcast and clear skies did not differ significantly due to the position of sun. This

result implies that the influence of irradiance on cavity and indoor temperature is weak due to the steep decrease in incoming irradiance that occurred because of the building's orientation.

Figure 5. Variation of outdoor irradiance (East-facing, Clear and overcast sky).
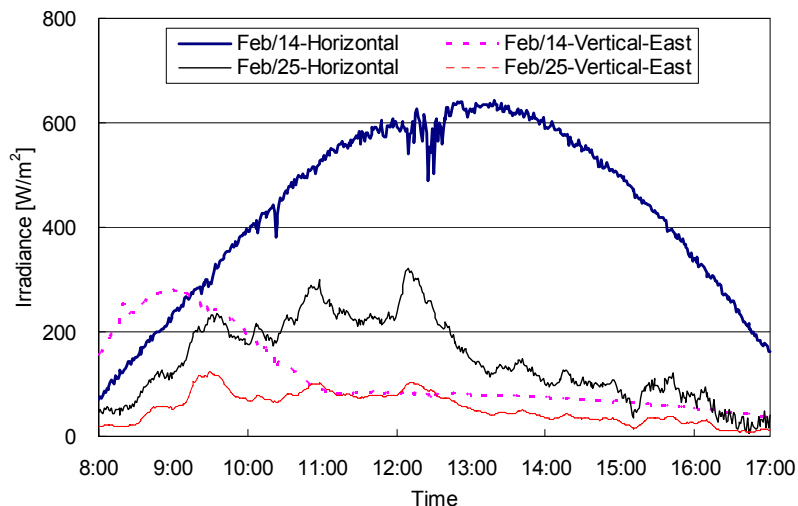
The variation in temperature for the selected days under clear and overcast skies is shown in Figures 6 and 7. Overall, the outdoor temperature during the daytime period under an overcast sky was lower than that under clear conditions. The lowest outdoor temperature was −10.5 °C during the nighttime in the absence of solar irradiance. The cavity temperature was higher than the indoor temperature when the vertical solar irradiance on the east-facing envelope was greatest. As the vertical solar irradiance diminished, the cavity temperature decreased below the indoor temperature since the openings installed at the bottom and top of the cavity allowed air to flow through cavity space without relatively being heated. Although the outdoor, indoor and cavity temperatures differed depending on the time of day and sky conditions, their variation patterns looked similar over the course of the monitoring periods. This result suggests that the change in indoor temperature is related to the outdoor and cavity temperatures.

Linear regression methods were employed in this study to examine the relationships between indoor temperature and thermal factors that influence changes in indoor temperature. Since the indoor temperature is influenced by various thermal factors that affect buildings, factors related to building thermal performance monitored in the field measurements were considered for inclusion in the regression models. Using the regression method, linear prediction models of the relationships between indoor temperature and thermal factors were developed for the various sky conditions considered in this study. Scatter plots for outdoor and indoor temperature were examined prior to determine appropriate regression for the relationship between them. The plot indicated that linear regression was a best suited for the relationship between outdoor and indoor temperature. Indoor temperature was the dependent variable and vertical irradiance arriving at the envelopes, outdoor temperature, and air temperature in the cavity space were used as independent variables in the respective models.

Figure 6. Variation of outdoor and cavity temperature (East-facing, 14 February, Clear sky).
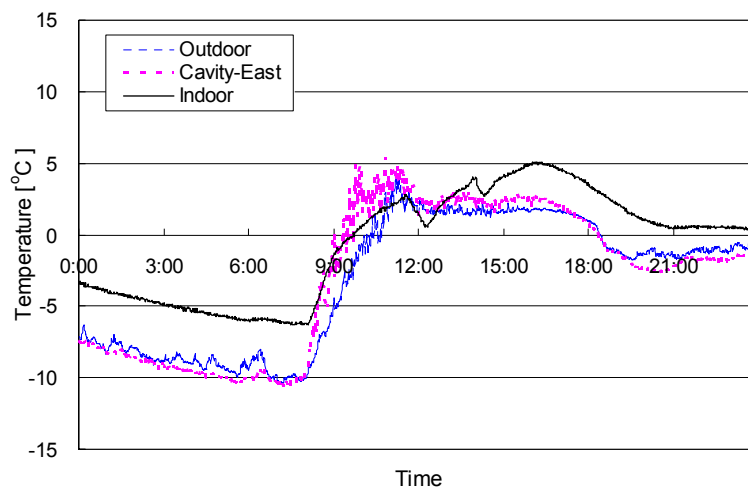
Figure 7. Variation of outdoor and cavity temperature (East-facing, 25 February, Overcast sky).
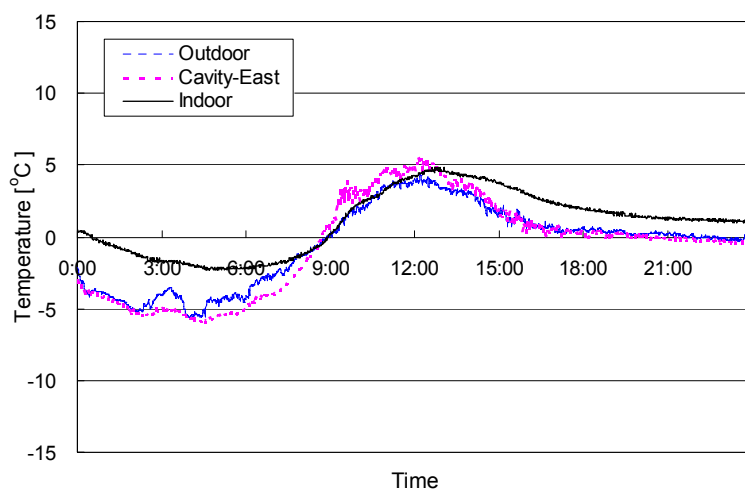
The relationship between indoor temperature and each variable during the monitoring periods is shown in Table 1, and a graph illustrating an example of a linear regression pattern for a day is shown in Figure 8. Overall, the results of the regression analyses imply that indoor temperature has a strong linear relationship with outdoor temperature and cavity temperature. ANOVA (ANalysis Of VAriance), which presents statistical analogousness between variables or groups, results indicated that the prediction models under all three sky conditions were significant at the 0.05 level.

The coefficient of determination for the models varied from 0.5802 to 0.8913, indicating that the reduced error variance in the indoor temperature vs. outdoor temperature or cavity models ranged from 58.02% to 89.13% for all three sky conditions considered in this study. This means that indoor temperature was effectively influenced by the outdoor temperature and cavity temperature under various sky conditions. In particular, the coefficient of determination was higher when the cavity temperature was included in the model.

Table 1. Linear regression models for indoor temperature (Winter, East-facing envelope).

Sky	Factor	Variables in model	Unstandardized coefficients		t	Sig.	r^2	ANOVA
			B	Std. Error				
Clear	Irradiance	(Constant)	3.1414	0.06	54.73	0.00	0.0853	$F(1,8815) = 821.76$,
		VA	−0.0140	0.00	−28.67	0.00		Sig. = 0.00
	Outdoor air	(Constant)	−0.5430	0.02	−24.78	0.00	0.7525	$F(1,8815) = 26796.74$,
		OA	0.5247	0.00	163.70	0.00		Sig. = 0.00
	Cavity	(Constant)	1.1041	0.02	68.69	0.00	0.7833	$F(1,8815) = 31817.91$,
		CA	0.8039	0.00	178.53	0.00		Sig. = 0.00
Partly cloudy	Irradiance	(Constant)	4.6924	0.12	38.40	0.00	0.0060	$F(1,2850) = 17.15$,
		VA	−0.0056	0.00	−4.14	0.00		Sig. = 0.00
	Outdoor air	(Constant)	0.5033	0.07	7.69	0.00	0.5802	$F(1,2850) = 3938.55$,
		OA	0.5118	0.01	62.76	0.00		Sig. = 0.00
	Cavity	(Constant)	0.8559	0.04	20.74	0.00	0.7598	$F(1,2850) = 9015.88$,
		CA	0.7993	0.01	94.95	0.00		Sig. = 0.00
Overcast	Irradiance	(Constant)	3.5199	0.07	51.79	0.00	0.0204	$F(1,5408) = 112.80$,
		VA	−0.0120	0.00	−10.62	0.00		Sig. = 0.00
	Outdoor air	(Constant)	1.5439	0.03	58.73	0.00	0.6221	$F(1,5408) = 8902.67$,
		OA	0.5171	0.01	94.35	0.00		Sig. = 0.00
	Cavity	(Constant)	1.2501	0.01	88.23	0.00	0.8913	$F(1,5408) = 44334.54$,
		CA	0.7265	0.00	210.56	0.00		Sig. = 0.00

Note: VA is Vertical irradiance; OA is Outdoor air temperature; CA is Cavity air temperature.

Figure 8. Relationship between outdoor air temperature and indoor air temperature (East-facing, daily data on 14 February only).
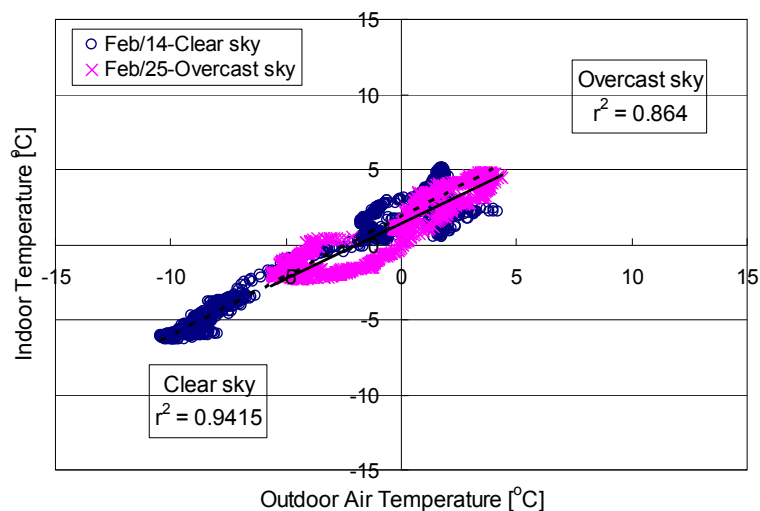
However, the relationship between indoor temperature and vertical irradiance arriving at the east-facing envelope was very weak due to the building orientation, under which a small amount of irradiance accumulated continuously during the data monitoring period. The coefficient of determination for this model ranged from 0.0060 to 0.0853, indicating that the error reduction of variance for the prediction model ranged from 0.6% to 8.53%. This result means that the reduction in error variance was insignificant. The ANOVA results confirmed this finding.

In summary, the influence of air temperature in the cavity space was stronger than the impact of outdoor air temperature. This implies that the cavity space had the greatest influence on the variation in indoor temperature. The influence of vertical solar irradiance reaching the envelope on indoor temperature appeared to be minimal based on the prediction of the indoor temperature of buildings with east-facing double skin envelopes.

3. Development of a New ANN Model

Based on the relationships discussed in the previous section, a new ANN model was developed using MATLAB, which is a numerical computing and programming software [9]. Its structure is illustrated in Figure 9. The new model was comprised of one input, one output, and four hidden layers. There were six, one, and ten neurons for the input, output, and hidden layers, respectively. The numbers of hidden layers and neurons were derived as optimal values in a previous study [1].

Solar radiation is related to the indoor temperature conditions and the reduction of the heating energy. Passive solar system such as solar greenhouses is a good example to understand energy saving effect in winter [11]. However, the amount of current solar radiation was not considered as one of the input variables for predicting future indoor temperature since, as describe in detail in the previous section, the relevance between the solar radiation and the indoor temperature was statistically low.

The reason for this irrelevance is, first, that the solar radiation does not exist during the nighttime, thus the indoor air temperature is not affected by the solar radiation for the nighttime. Secondly, during the daytime as well, the amount of solar radiation fluctuates by the cloud conditions. However, the indoor temperature cannot respond fast to that fluctuation. Therefore, the solar radiation was not selected as an input variable in this ANN model.

Input values for the input neurons were normalized to be between 0 and 1. Normalized values were represented as $TEMP_{IN}$ (from −10 °C to 40 °C), $\Delta TEMP_{IN}$ (from −10 °C to 10 °C), $TEMP_{OUT}$ (from −20 °C to 40 °C), $TEMP_{CAV}$ (from −20 °C to 80 °C), opening conditions of the internal skin (opened: 1 or closed: 0), and opening conditions of the external skin (opened: 1 or closed: 0). One output neuron ($TEMP_{PR}$) was calculated to produce the future indoor air temperature. The Tangent-Sigmoid transfer function was employed between the input and hidden layers, and the pure linear transfer function and was employed between the hidden and output layers.

The parameters for model training were a 0.75 learning rate, 0.30 moment, 43 training data sets, and the Levenberg-Marquardt algorithm. The values for learning rate and moment were taken from a previous study [1]. In addition, the training goal was set to 0.01 K^2 (mean square of errors). The measured data from actual buildings described in Section 2 were used for the training data set. For the model, the number of data sets was determined by Equation (1) [12]:

$$N_d = (N_h − 1/2 \times (N_i + N_o))^2 \qquad (1)$$

The training process was iteratively conducted when a new training data set was provided. For this iterative training process, the sliding window method was used as a data managing technique. Thus, when a new training data set was newly added to the existing data sets, the oldest one was removed to better reflect the new set.

Figure 9. Structure of a new ANN model.
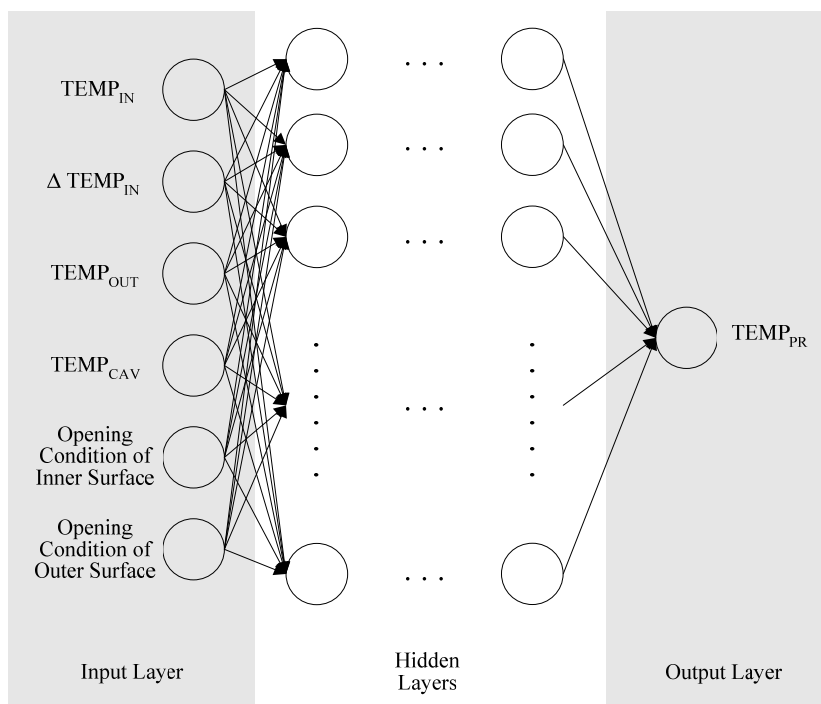
4. Optimization of the New ANN Model

A parametrical optimization process was utilized for the structure and learning methods of the new ANN model. Based on the optimal number of hidden layers, the number of neurons in the hidden layers, the learning rate and moment, the optimized ANN model was expected to produce more accurate and stable outputs. Data measured in the building with a double skin envelope described in Section 2 were used as the data set for the optimization process.

The optimal structure and learning methods were determined by comparing the difference in the root mean square (RMS) between monitored values from the actual building and predicted values from the ANN model. The parameter with the least RMS was chosen as the optimal method. Before each optimization step, the weights between neurons were initialized again to prevent the previous optimization process from influencing the results.

The first parameter to be optimized was the number of hidden layers. RMS(s) ranging from 1 to 10 were compared in this step. During the first optimization step, the number of neurons in the hidden layers, learning rate, and moment were fixed as in the initial model. All ten models with different numbers of hidden layers predicted the future indoor temperature conditions stably, therefore the RMS values of the errors were all smaller than the designated training goal (RMS: 0.1 K, MSE: 0.01 K^2). The model with six hidden layers had the lowest RMS of 0.03735 K, and thus six was deemed the optimum number of hidden layers.

The second parameter was the number of neurons in the hidden layers. Models with different numbers of neurons in each hidden layer ranging from 10 to 20 were compared. During this step, the number of hidden layers was fixed at six based on the previous step, and values for learning rate and moment were the same as in the initial model. All models had stable RMS values that satisfied the

training goal. The minimum, and therefore optimum, value of 0.03735 K was achieved by a model with 13 hidden layer neurons.

The third and fourth parameters were the learning rate and moment, respectively. ANN models with from 0.00 to 1.00 and a 0.05 increase in size for each parameter were tested. The optimum number of hidden layers (6) and the number of hidden layer neurons (13) were applied for these steps. The optimum learning rate and moment were 0.55 (RMS 0.03705 K) and 0.25 (RMS 0.03647 K), respectively. Based on this optimization process, the optimal structure and learning methods for the ANN model was determined to be 6 hidden layers, 13 neurons in the hidden layers, a 0.55 learning rate, and moment of 0.25.

## 5. Performance Tests of the Optimized ANN Model

5.1. Description of the Performance Tests

Performance tests of the optimized ANN model were conducted using a numerical simulation. TRNSYS [13] and MATLAB [9] tools were incorporated for the simulation. This software package was employed to model the practical conditions of the actual double skin building used for field measurements, and calculate the indoor temperature ($TEMP_{IN}$) of the building. The conditions included building properties and related components such as heating and cooling systems, internal load, ventilation rates, initial thermal conditions and weather data.

The calculated air temperature was used in MATLAB for numerical computing and programming. MATLAB was effective for developing an ANN model and calculating future indoor temperature ($TEMP_{PR}$) by the ANN model. It also functioned to determine the most efficient operation of the heating and cooling systems, and the optimal opening strategies of the double skin envelopes. Decisions for the temperature control systems and opening configurations based on the results from MATLAB were fed into the TRNSYS in order to operate the heating and cooling systems and envelope opening. Then, a new indoor temperature from the TRNSYS was used in MATLAB. This process was iterated at every control cycle. In addition, when a new training data set is acquired, it is added to the training sets removing oldest one.

The validity of the combined simulation method was proven in a previous study conducted by Moon *et al.* [1,2]. In that study, indoor temperatures predicted using an ANN model were compared with the indoor temperatures determined from monitoring the existing building. The RMS of the difference between them was 0.0259 K, smaller than the designated goal of 0.1 K RMS. This finding means that these simulation tools can be used to successfully conduct performance tests on the developed ANN model.

The developed ANN-based logic and the non-ANN counterpart were applied in the test building described in Figure 10 and Table 2. The non-ANN-based logic, which represented the conventional logic, was designed to turn on the heating or cooling systems when the indoor air temperature was outside the specified comfort range.

Figure 10. Layout of a tested building: (**a**) Plan; (**b**) Front elevation; (**c**) Section (unit: mm).

(**a**)　　　　　　　　　　　(**b**)　　　　　　　　　　　(**c**)
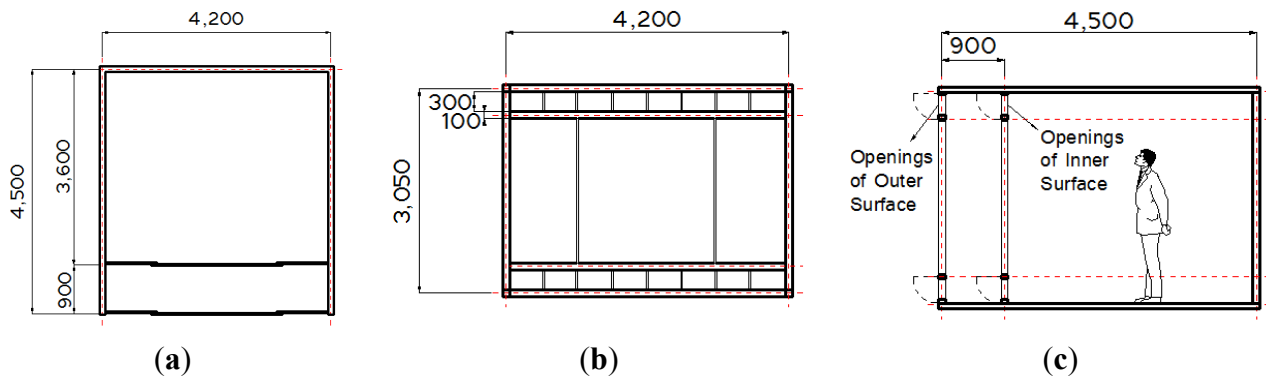
Table 2. Descriptions of a test building.

Location for Weather Data	Seoul, South Kroea (latitude: 37.56° N, longitude: 126.98° E)	
Spcae Configuration	Dimension: 4.2 m (width) × 4.5 m (depth) × 3.05 m (height)	
	Total area: 18.9 m^2 (Indoor area: 15.12 m^2, Cavity area:3.78 m^2)	
Envelope Insulation (°K m^2/W) [14]	Walls	2.78
	Roof	5.00
	Floor	2.44
	Windows	0.18 for the external envelope (24 mm clear glass)
		0.77 for the internal envelope
		(6 mm gray glass + 16 mm argon gas + 6 mm gray glass)
	Doors	0.2
Internal Gain	2 seated, light work, typing occupants	
	2 computers with printer	
	5 W/m^2 lighting fixtures	
Infiltration Rate [15]	0.7 ACH	
Systems Applied [15]	Radiative heating: 7172 kJ/h heat supply	
	Convective cooling: 6315 kJ/h heat removal	
System Operation Ranges [16]	Heating: 20–23 °C	
	Cooling: 23–26 °C	

Four control options for the openings installed in the envelopes were independently applied in the control logic. The first option was closure of the openings in both the internal and external envelopes (case 1). The second option was closure of the opening in the internal envelope and opening of that in the external envelope (case 2). The third option was closure of the opening in the external channels and opening of that in the internal envelope are (case 3). The last option was leaving both internal and external envelopes open (case 4).

Performance tests were conducted for two weeks selected from the heating and cooling seasons. The test results obtained during the first week were not considered in the primary analysis results since the ANN model needed to adapt to the test building. The test results for the second week are primarily discussed in this study.

5.2. Result Analysis

The conditions influencing the indoor air temperature in the winter determined by the ANN-based logic and non-ANN-based logic for the four opening strategies are compared in Figures 11–14. The comfortable periods of indoor temperature, mean temperature, and the amount of heat supplied according to the two types of logic are summarized in Table 3.

For the case 1, where both the internal and external envelopes were closed, the adjustment of indoor temperatures by the ANN-based logic and non-ANN-based logic showed similar patterns (Figure 11). This finding suggests that the logic employed to predict temperature using the ANN worked properly. Furthermore, the length of the comfortable indoor temperature period increased by about 0.12% for the test period when the ANN-based logic was used (Table 3). In particular, cold periods due to undershooting by the heating system did not exist. The average temperature determined by the ANN-based logic was 0.18 °C, higher, thus more heat had to be supplied indoors.

Figure 11. Profiles of the indoor air temperature for case 1 in winter (8–14 January) (Case 1—Opening at internal envelope: closed, Opening at external envelope: closed).
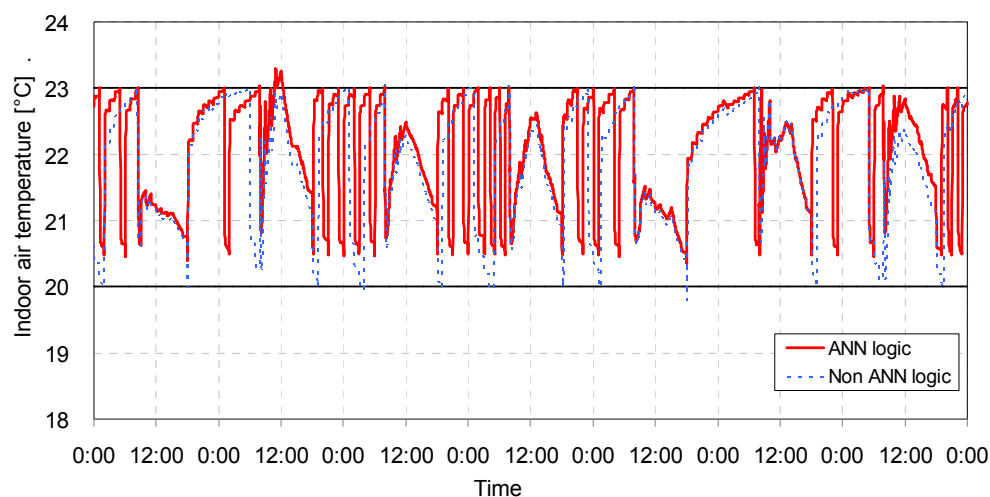
The indoor air temperature profile for case 2 is shown in Figure 12. The number of system on/off cycles decreased due to the scanty insulation of the envelopes. Since the opening at the external envelope was opened, the thermal buffer zone in the cavity space did not function effectively. It therefore took more time to heat the indoor space to the upper limit of the comfort range, which was assumed to be 23 °C in this study.

Regarding temperature stability, the ANN-based logic provided similar or slightly more stable temperature conditions compared with those provided by the non-ANN-based logic (Table 3). Similar to the previous case, the degree of fluctuation was less significant with the predictive logic, thus the comfortable period was extended by 0.09%. The amount of heat supplied by the ANN-based logic was larger than that supplied by the conventional logic because the indoor temperature was conditioned as much as 0.31 °C higher compared to the non-ANN-based logic.

Figure 12. Profiles of the indoor air temperature for case 2 in winter (8–14 January) (Case 2—Opening at internal envelope: closed, Opening at external envelope: opened).
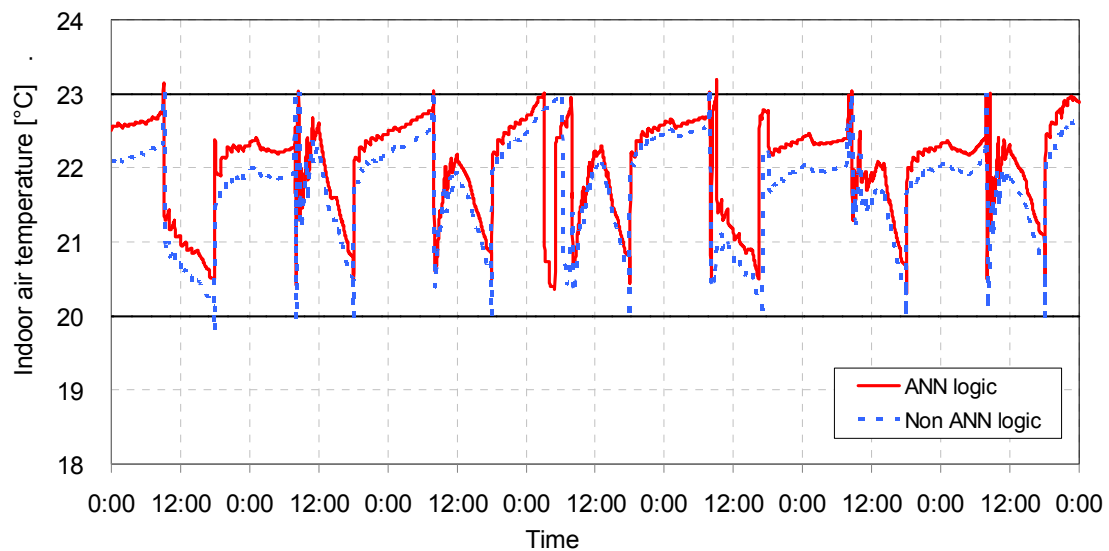

Table 3. Performance of the ANN-based logic and non-ANN-based logic in winter (8–14 January).

Case	Opening conditions		ANN model application	Comfortable period in percentile	Uncomfortable period in percentile		Average temperature (°C)	Amount of heat supply (KJ)
	Internal envelope	External envelope			Over comfort range	Under comfort range		
1	Closed	Closed	No	99.78	0.10	0.12	21.89	548,538
			Yes	99.90	0.10	0.00	22.07	555,830
2	Closed	Open	No	99.81	0.09	0.10	21.74	709,669
			Yes	99.90	0.10	0.00	22.05	719,232
3	Open	Closed	No	64.27	0.07	35.66	20.44	1,072,214
			Yes	66.34	0.00	33.66	20.48	1,078,669
4	Open	Open	No	0.01	-	99.99	7.91	1,204,896
			Yes	0.01	-	99.99	7.91	1,204896

Figure 13 shows the indoor air temperature in case 3, where the internal envelope was opened and the external envelope was closed. In this case, the thermal buffer zone formed by the enclosed cavity space was removed due to the airflow through the opening in the internal envelope. In addition, the actual insulation level of the external envelope was lower than that in case 2 since the insulation capability of the external envelope is weaker than that of the internal envelope. Thus, the number of heating system on/off cycles was reduced because more time was required to heat up the indoor space.

Figure 13. Profiles of the indoor air temperature for case 3 in winter (8–14 January). (Case 3—Opening at internal envelope: opened, Opening at external envelope: closed).
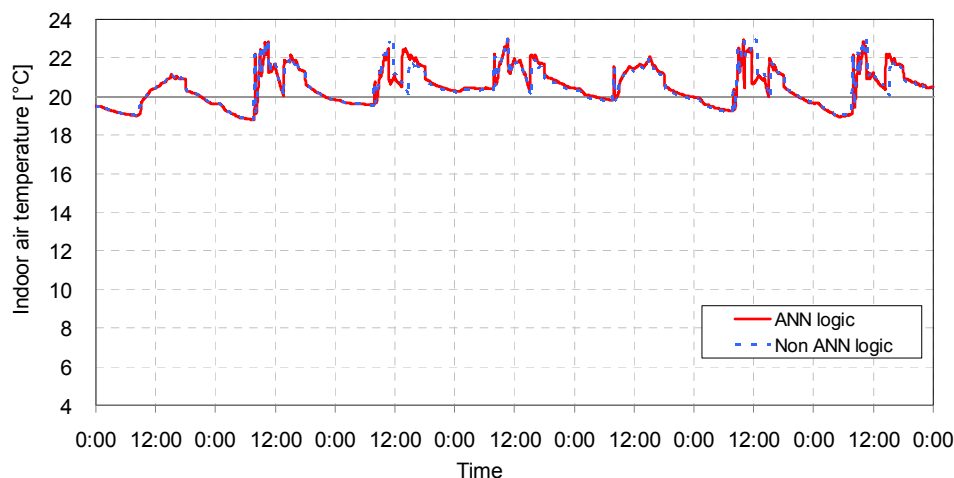
For the temperature conditions, both types of control logic yielded similar results, but the duration of the comfortable period was markedly increased by 2.07% when the ANN-based logic was used (Table 3). Both types of logic created a significantly uncomfortable cold period comprising 30% of the total period. This was not due to a logic malfunction, but the insufficient capacity of the heating system. Even when the heating system was working, the indoor temperature dropped under the lower limit of the comfort range, which was 20 °C in this study. This phenomenon was also related to the weaker insulation capability of the external envelope. Similar to cases 1 and 2, the average indoor temperature maintained by the ANN-based logic was higher than that maintained by conventional logic. The difference between them was 0.04 °C and more heat was supplied to the space.

With case 4, where the internal and external envelopes were both opened, the temperature profiles determined by the ANN-based logic and non-ANN-based logic were identical. The variation pattern of the profiles is shown in Figure 14. The variation was due to the direct supply of cold outdoor air to the indoor space through the openings in envelopes. The indoor temperature failed to reach the comfort range despite the fact that the heating system worked according to schedule. Accordingly, the comfortable period under this condition was zero. As shown in Table 3, the average temperature and the amount of heat supplied to the indoor space were equal.

A comparative performance analysis of the ANN-based logic and non-ANN-based logic was conducted for the four opening strategies during the summer. The results are shown in Figures 15–19 and Table 4. As presented in Figures 15 and 17, the indoor air temperature conditions for case 1 and 2 were relatively well stabilized within the comfort range, which was between 23 °C and 26 °C in this study. Figure 16 magnifies the temperature profile for case 1. At every on/off cycle of system, the overshoot and undershoot by the non-ANN based logic went out of the comfort range, while those of the ANN-based logic maintained the indoor temperature within the comfort range.

Figure 14. Profiles of the indoor air temperature for case 4 in winter (8–14 January). (Case 4—Openings at internal envelope: opened, Opening at external envelope: opened).
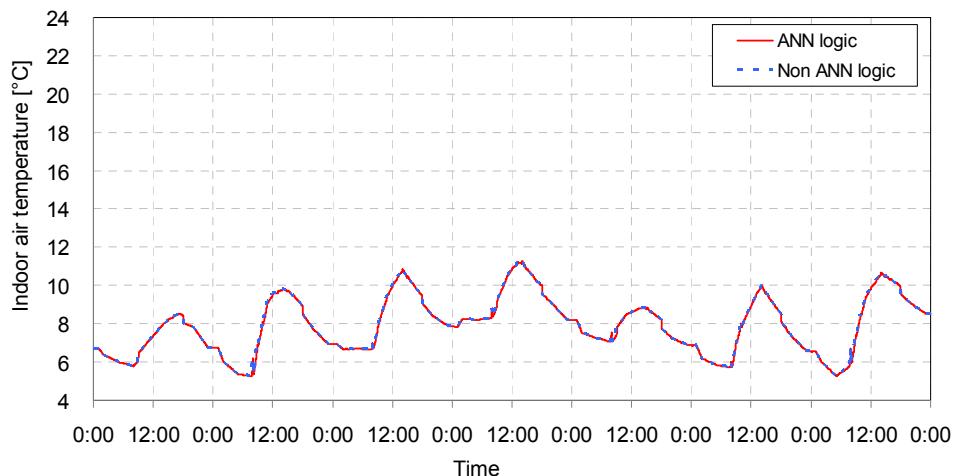

Figure 15. Profiles of the indoor air temperature for case 1 in summer (8–14 August). (Case 1—Opening at internal envelope: closed, Opening at external envelope: closed).
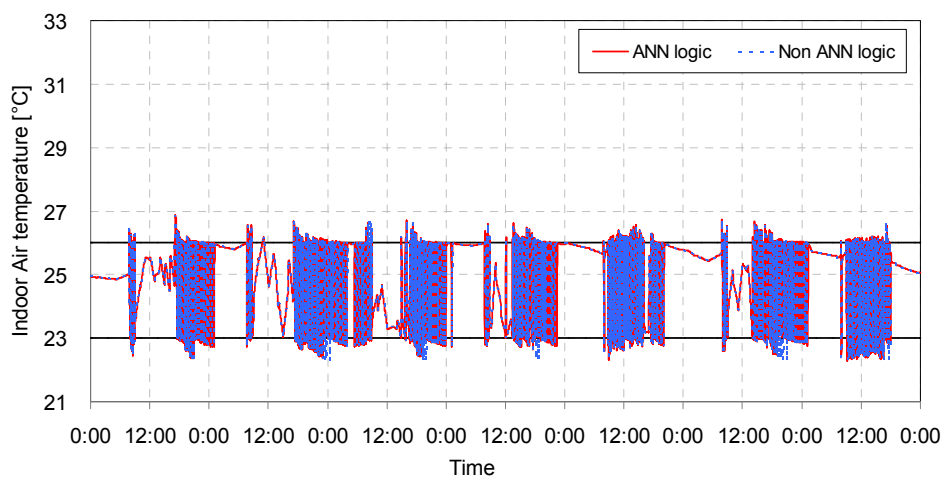

Figure 16. Profiles of the indoor air temperature for case 1 on a summer day (11 August only). (Case 1—Opening at internal envelope: closed, Opening at external envelope: closed).
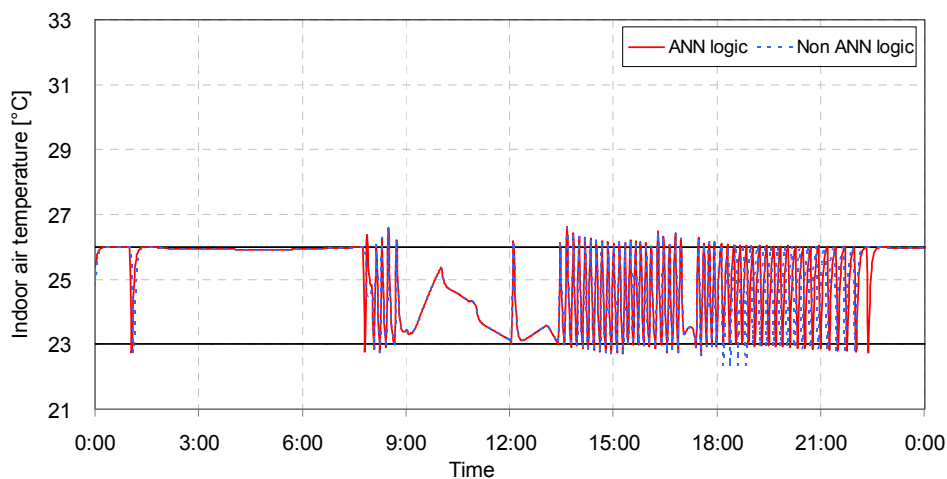
Figure 17. Profiles of the indoor air temperature for case 2 in summer (8–14 August). (Case 2—Opening at internal envelope: closed, Opening at external envelope: opened).
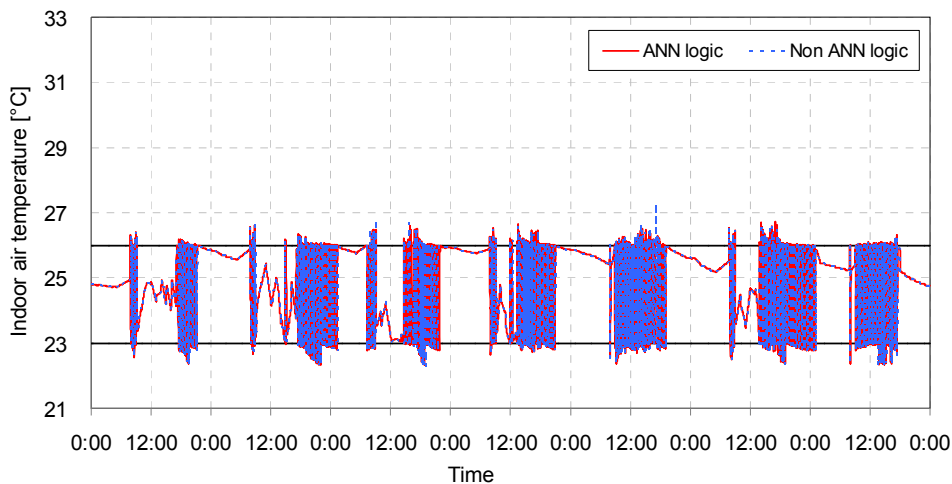

Figure 18. Profiles of the indoor air temperature for case 3 in summer (8–14 August). (Case 3—Opening at internal envelope: opened, Opening at external envelope: closed).
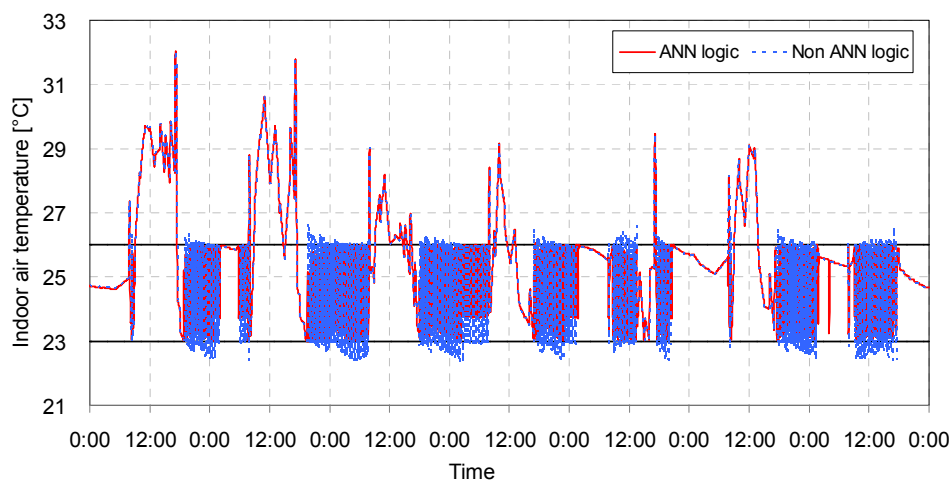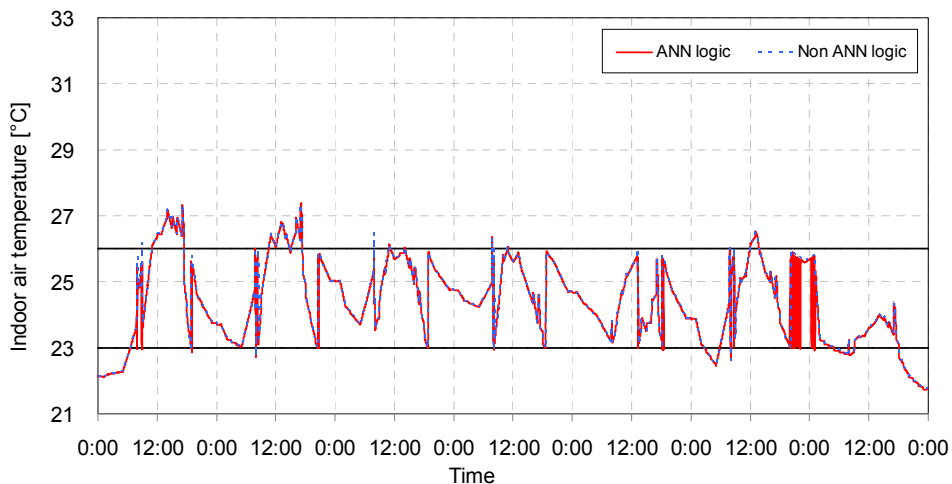

Figure 19. Profiles of the indoor air temperature for case 4 in summer (8–14 August). (Case 4—Opening at internal envelope: opened, Opening at external envelope: opened).

The comfortable indoor temperature periods were increased by the ANN-based method by as much as 0.68% for case 1 and 0.20% for case 2. The amount of heat removed in case 1 was reduced although the average indoor temperatures for the two types of logic were nearly the same. On the other hand, as shown in Table 4, it was slightly increased for case 2 due to the lower average indoor temperature.

For case 3, where the internal envelope was opened and the external envelope was closed, the comfortable periods provided by both control logics were significantly reduced due to the weak envelope insulation. As shown in Figure 18, the indoor temperature was out of the comfort range during the daytime even when the cooling system was working. The comfortable periods for the ANN-based logic and non-ANN-based logic were 80.60% and 72.60%, respectively, indicating that the ANN-based logic created an 8.0% longer comfortable period than the non-ANN based logic. It is also shown in Table 4 that the ANN-based logic required 239 kJ less heat to be removed for space cooling than did the non-ANN-based logic.

Table 4 shows the comfortable periods for case 4, where the openings in the internal and external envelopes were both opened. The overall comfortable periods maintained by the ANN-based and non-ANN-based types of logic were 79.02% and 79.00%, respectively. Temperatures that may cause thermal discomfort occurred in the early morning and during the daytime as shown in Figure 19. The indoor temperature in early morning dropped below the comfort range due to penetration of the cold air from outside, and the indoor temperature during the day rose above the comfort range even though the cooling system was working. The improvement achieved by the ANN-based logic was 0.02%, but the ANN-based logic required more heat to be removed due to the lower average indoor temperature.

Based on the analysis of the temperature conditions for winter and summer, it was concluded that the ANN-based logic created more stable indoor temperature conditions with increased comfortable periods and decreased overshoot and undershoot out of the comfort range. The findings discussed in this study support the potential of applying the ANN model to the control logic based on its prediction accuracy and adaptability.

Table 4. Performance of the ANN-based logic and non-ANN-based logic in summer (8–14 August).

Case	Opening conditions		ANN model application	Comfortable period in percentile	Uncomfortable period in percentile		Average temperature (°C)	Amount of heat removal (kJ)
	Internal envelope	External envelope			Over comfort range	Under comfort range		
1	Closed	Closed	No	90.11	4.57	5.32	24.98	956,625
			Yes	90.79	4.32	4.89	24.98	956,386
2	Closed	Open	No	92.36	3.57	4.07	24.97	851,555
			Yes	92.56	3.52	3.92	24.96	852,392
3	Open	Closed	No	72.60	23.05	4.36	25.62	1,222,348
			Yes	80.60	19.39	0.00	25.61	1,222,109
4	Open	Open	No	79.00	9.37	11.63	24.66	945,389
			Yes	79.02	9.23	11.76	24.62	969,415

6. Conclusions

This study aimed at developing an ANN model that is reliable with respect to the relationship between input and output variables. A new ANN model was developed followed by an optimization process. The performance of the optimized ANN model was tested for diverse opening strategies in heating and cooling seasons. A summary of the findings of this study is provided below:

(1) The primary influential thermal factors affecting the prediction of indoor temperature by the new ANN models developed in this study were the outdoor and cavity temperatures since they were significantly related to the indoor temperature of an actual double-skinned building in summer and winter. The vertical solar irradiance reaching the envelopes was excluded from the new ANN model since the statistical correlation between indoor temperature and solar irradiance was insignificant. This implies that thermal factors generally used for input variables in prediction models should be prescreened in order to improve the prediction accuracy of the ANN-based model.

(2) The new ANN model was parametrically optimized in terms of the root mean square (RMS) of the difference between the predicted data from the ANN model and the monitored data from an existing building. The optimized ANN model, which had six hidden layers, 13 neurons in the hidden layers, a 0.55 learning rate, and a moment of 0.25, predicted the future indoor temperature more accurately and stably.

(3) The performance tests of the optimized ANN model-based control logic for four different opening strategies of a double skin envelope during the heating and cooling seasons revealed that the ANN-based logic yielded an improved indoor temperature environment compared to that provided by the non-ANN based logic. The overall comfortable temperature period maintained by ANN-based control increased with reduced frequencies of overshoots and undershoots out of the comfort range. However, the amount of heat supplied during the heating season and heat removed during the cooling season was not significantly reduced by the ANN-based logic.

The results of this study imply that optimally modified ANN models have the potential to be successfully applied in temperature control logic for buildings with double skin envelopes. The ANN model proposed in this study was able to predict future indoor temperatures for diverse envelope opening strategies. Thus, based on the predicted future temperatures, the control logic can efficiently determine the operation of heating and cooling systems as well as the opening configurations of the double skin envelope in terms of thermal comfort and energy savings.

This study was performed under the limited conditions of field measurements and the limited boundaries of the two types of control logic. Building energy efficiency achieved by the application of the ANN-based model was not examined in this study. Further studies are necessary to investigate the performance of the ANN-based temperature control logic in a real building environment in order to examine the effect of energy savings and work productivity under the improved thermal environment.

The effect of shading devices in the double skin envelope was not considered in this study. The developed ANN model needs to employ the status of the shading device as one of the input variables or the operation of the shading device could be determined in the rule-based control logic. Further study regarding this issue is warranted in the future.

An ANN model for predicting indoor PMV or PPD values must be valuable to be developed. For this, a variety of additional input variables are required such as humidity, mean radiant temperature, air

movement, and occupant's activity and clothing level. The simplified model will be necessary, and once the PMV predicting ANN model and control logic was developed, it must be very helpful to provide an overall thermal comfort to the occupants.

In addition, cavity temperature in real situations is influenced by outdoor temperature and variation of solar irradiance during daytime. In some sense, the variation of cavity temperature needs to be predicted in advance in order to predict indoor temperature. In this study, the cavity temperature was not predicted but monitored in field measurements. For the prediction of indoor temperature, the monitored cavity temperature functioned as an independent variable, where the influence of solar irradiance and outdoor temperature was reflected. In future study, prediction models to calculate cavity temperature based on surrounding thermal components, such as irradiance and outdoor temperature need to be considered.

Acknowledgments

Conflicts of Interest

The authors declare no conflict of interest.

References

1. Moon, J.W.; Yoon, S.H.; Kim, S. Development of an artificial neural network model based thermal control logic for double skin envelopes in winter. *Build. Environ.* **2013**, *61*, 149–159.
2. Moon, J.W.; Chang, J.D.; Kim, S. Artificial Neural Network for Controlling the Openings of Double Skin Envelopes and Cooling Systems. In Proceedings of the 2012 International Conference on Sustainable Design and Construction: Fort Worth, TX, USA, 2012; pp. 81–89.
3. Kim, Y.M.; Lee, J.H.; Kim, S.M.; Kim, S. Effect of double skin envelopes on natural ventilation and heating loads in office buildings. *Energy Build.* **2011**, *43*, 2118–2126.
4. Kim, Y.M.; Sohn, J.Y.; Shin, S.W.; Kim, S. Contribution of natural ventilation in a double skin envelope to heating load reduction in winter. *Build. Environ.* **2009**, *44*, 2235–2244.
5. Baldinelli, G. Double skin facades for warm climate regions: Analysis of a solution with an integrated movable shading system. *Build. Environ.* **2009**, *44*, 1107–1118.
6. Yoon, S.H.; Park, C.S. Control levels of a double skin façade. *J. Archit. Inst. Korea Plan. Des.* **2010**, *26*, 307–326.
7. Gratia, E.; De Herde, A. Natural cooling strategies efficiency in an office building with a double-skin façade. *Energy Build.* **2004**, *36*, 1139–1152.
8. Moon, J.W.; Kim, S. Artificial neural network for the control of the openings and cooling systems of the double skin envelope buildings. *Adv. Mater. Res.* **2013**, *610*, 2859–2865.

9. MathWorks. MATLAB 14. Available online: http://www.mathworks.com (accessed on 17 October 2008).

10. Moon, J.W.; Kim, S. Application of artificial neural network for optimum controls of windows and heating systems of double-skinned buildings. *Korean J. Air-Condit. Refrig. Eng.* **2012**, *8*, 627–635.

11. Asdrubali, F.; Cotana, F.; Messineo, A. On the evaluation of solar greenhouse efficiency in building simulation during the heating period. *Energies* **2012**, *5*, 1864–1880.

12. Kalogirou, S.A.; Bojic, M. Artificial neural networks for the prediction of the energy consumption of a passive solar building. *Energy* **2000**, *25*, 479–491.

13. University of Wisconsin. TRNSYS16.1. Available online: http://sel.me.wisc.edu/trnsys/ (accessed on 10 December 2010).

14. *Design of Environmental-Friendly Houses and Guidelines for Performance Evaluation*; Ministry of Land, Transport and Maritime Affairs: Gwacheon, Korea, 2009.

15. Alpine. Sizing Estimator for Heating & Cooling Equipment. Available online: http://www.alpinehomeair.com/view.cfm?objID=4A176770-C3EB-4E97-AAED-C34B81D7AFED (accessed on 23 November 2012).

16. American Society of Heating, Refrigerating and Air Conditioning Engineers (ASHRAE). *Energy-Efficient Design of Low-Rise Residential Buildings*; ANSI-ASHRAE Standard 90.2-2004; ASHRAE: Atlanta, GA, USA, 2004.